

SHOC2 mRNA is abundant in adult testis and immune tissues as well as in fetal brain. The C>A>G (p.S2G) mutation was not detected in 82 samples from patients with leukemia.

Clinical manifestations in SHOC2 mutation-positive patients often vary, even among patients who have a common p.S2G mutation (Table 2 and Supplementary Table 4). In this study and in a previous study, relative macrocephaly (94%), hypertelorism (79%), low-set ears (91%) and short stature (100%) were frequently observed in patients with the SHOC2 p.S2G mutation.¹⁸ Growth hormone deficiency was observed in 70% of patients. With respect to cardiac abnormalities, pulmonary stenosis was observed in 13 of 33 patients (39%), followed by atrial septal defect (33%), mitral valve anomaly (31%) and hypertrophic cardiomyopathy (27%). Dark skin and atopic dermatitis were seen in 75 and 48% of patients, respectively. Hair abnormalities, including sparse hair (100%) and loose anagen hair/easily pluckable hair (100%), were the most characteristic clinical features of SHOC2 mutation-positive patients.

The symptomatology of patients with the SHOC2 mutation does not fit existing disorders, including Noonan, Costello and CFC syndrome. In this paper, we summarize the clinical manifestations of patients with CFC syndrome^{21,22} or Noonan syndrome,²³ as described in previous reports, as well as SHOC2 mutation-positive patients (Table 2). The high frequencies of mental retardation (84%) and sparse hair (100%) observed in SHOC2 mutation-positive patients are similar to those observed in CFC patients (100 and 89%, respectively); the frequency of mental retardation was higher than that in patients with Noonan syndrome (42%). With respect to cardiac abnormalities, the frequencies of hypertrophic cardiomyopathy, atrial septal defect and mitral valve anomaly are similar to those among patients with Noonan syndrome. However, pulmonary stenosis (39%) was less frequent in SHOC2 mutation-positive patients than in patients with Noonan syndrome (63%). It is of note that short stature (100%) and pectus deformity (72%) were found to be most frequent in patients with the SHOC2 mutation. Furthermore, loose anagen/easily pluckable hair has not been reported in mutation-positive patients with Noonan, CFC or Costello syndrome. Taken together, these results suggest that clinical manifestations in patients with SHOC2 partially overlap with those of Noonan syndrome and CFC syndrome. The presence of easily pluckable/loose anagen hair is distinctive in SHOC2 mutation-positive patients.

Loose anagen hair has been observed in an isolated loose anagen hair syndrome (OMIM 600628)²⁴ and has been found to be associated with Noonan syndrome.^{25,26} The pathogenesis of loose anagen hair remains unknown. A scalp biopsy in a patient with loose anagen hair showed marked cleft formation between the inner root and the irregularly shaped hair shafts. Abnormalities in the keratin gene have been suggested.²⁴ Functional analysis of the SHOC2 p.S2G mutant showed that the mutant protein was aberrantly localized in the membrane fraction after stimulation with epidermal growth factor and induced extracellular signal-regulated kinase signaling in a cell-specific manner.¹⁸ It is possible that dysregulated proliferation or cell-to-cell attachment causes the detachment between inner sheaths and hair shafts.

One of our mutation-positive patients exhibited a remarkable leukocytosis ranging from 12 000 to 24 600/mm³. Other patients also showed mild leukocytosis, which is near the upper range of the normal levels for their age. This observation led us to examine the tissue and cellular expression of SHOC2. In adult tissues, the highest SHOC2 expression was observed in testis; relatively high expression was also observed in several immune tissues, including spleen, bone marrow, tonsil and lymph node. Among leukocytes, the expression of

SHOC2 was six times higher in PMN than in mononuclear, suggesting that SHOC2 might be important to the proliferation or survival of PMN leukocytes. We did not identify the p.S2G mutation in 82 samples from patients with hematologic malignancies. A recent study reported that no SHOC2 mutations were identified in 22 patients with juvenile myelomonocytic leukemia.²⁷ It is possible that the absence of mutation was due to the relatively small sample size. Alternatively, the gain of function of SHOC2 might not have leukemogenic potential, and other factors such as aberrant cytokine production may be associated with leukocytosis.

In summary, we identified the SHOC2 p.S2G mutation in eight patients with Noonan-like syndrome. Analysis of the detailed clinical manifestations of these patients showed that relative macrocephaly, hypertelorism, low-set ears, short stature, sparse/easily pluckable hair and a variety of skin abnormalities, including dark skin and atopic dermatitis, are frequently observed in patients positive for this mutation. A previous study and this study show that only one mutation (p.S2G) is causative for the phenotype. The rapid detection system for the SHOC2 p.S2G mutation using the Lightcycler will be a useful tool to screen for this mutation in patient samples.

ACKNOWLEDGEMENTS

We thank the patients and families who participated in this study as well as the doctors who referred the patients. This work was supported by Grants-in-Aids from the Ministry of Education, Culture, Sports, Science and Technology of Japan, Japan Society for the Promotion of Science and The Ministry of Health Labour and Welfare to YM and YA.

- Allanson, J. E., Hall, J. G., Hughes, H. E., Preus, M. & Witt, R. D. Noonan syndrome: the changing phenotype. *Am. J. Med. Genet.* **21**, 507–514 (1985).
- van der Burg, I. Noonan syndrome. *Orphanet. J. Rare Dis.* **2**, 4 (2007).
- Hennekam, R. C. Costello syndrome: an overview. *Am. J. Med. Genet. C Semin. Med. Genet.* **117**, 42–48 (2003).
- Reynolds, J. F., Neri, G., Herrmann, J. P., Blumberg, B., Coldwell, J. G., Miles, P. V. et al. New multiple congenital anomalies/mental retardation syndrome with cardio-facio-cutaneous involvement—the CFC syndrome. *Am. J. Med. Genet.* **25**, 413–427 (1986).
- Aoki, Y., Niihori, T., Narumi, Y., Kure, S. & Matsubara, Y. The RAS/MAPK syndromes: novel roles of the RAS pathway in human genetic disorders. *Hum. Mutat.* **29**, 992–1006 (2008).
- Bentires-Alj, M., Kontaridis, M. I. & Neel, B. G. Stops along the RAS pathway in human genetic disease. *Nat. Med.* **12**, 283–285 (2006).
- Pandit, B., Sarkozy, A., Pennacchio, L. A., Carta, C., Oishi, K., Martinelli, S. et al. Gain-of-function RAF1 mutations cause Noonan and LEOPARD syndromes with hypertrophic cardiomyopathy. *Nat. Genet.* **39**, 1007–1012 (2007).
- Razzaque, M. A., Nishizawa, T., Konioke, Y., Yagi, H., Furutani, M., Aono, R. et al. Germline gain-of-function mutations in RAF1 cause Noonan syndrome. *Nat. Genet.* **39**, 1013–1017 (2007).
- Roberts, A. E., Araki, T., Swanson, K. D., Montgomery, K. T., Schiripo, T. A., Joshi, V. A. et al. Germline gain-of-function mutations in SOS1 cause Noonan syndrome. *Nat. Genet.* **39**, 70–74 (2007).
- Schubbert, S., Zenker, M., Rowe, S. L., Boll, S., Klein, C., Bollag, G. et al. Germline KRAS mutations cause Noonan syndrome. *Nat. Genet.* **38**, 331–336 (2006).
- Tartaglia, M., Mehler, E. L., Goldberg, R., Zampino, G., Brunner, H. G., Kremer, H. et al. Mutations in PTPN11, encoding the protein tyrosine phosphatase SHP-2, cause Noonan syndrome. *Nat. Genet.* **29**, 465–468 (2001).
- Tartaglia, M., Pennacchio, L. A., Zhao, C., Yadav, K. K., Fodale, V., Sarkozy, A. et al. Gain-of-function SOS1 mutations cause a distinctive form of Noonan syndrome. *Nat. Genet.* **39**, 75–79 (2007).
- Aoki, Y., Niihori, T., Kawane, H., Kurokawa, K., Ohashi, H., Tanaka, Y. et al. Germline mutations in HRAS proto-oncogene cause Costello syndrome. *Nat. Genet.* **37**, 1039–1040 (2005).
- Niihori, T., Aoki, Y., Narumi, Y., Neri, G., Cave, H., Verioles, A. et al. Germline KRAS and BRAF mutations in cardio-facio-cutaneous syndrome. *Nat. Genet.* **38**, 294–296 (2006).
- Rodriguez-Viciana, P., Tetsu, O., Tidyman, W. E., Estep, A. L., Conger, B. A., Cruz, M. S. et al. Germline mutations in genes within the MAPK pathway cause cardio-facio-cutaneous syndrome. *Science* **311**, 1287–1290 (2006).

- 16 Selfors, L. M., Schutzman, J. L., Borland, C. Z. & Stern, M. J. soc-2 encodes a leucine-rich repeat protein implicated in fibroblast growth factor receptor signaling. *Proc. Natl Acad. Sci. USA* **95**, 6903–6908 (1998).
- 17 Rodriguez-Viciana, P., Oses-Prieto, J., Burlingame, A., Fried, M. & McCormick, F. A phosphatase holoenzyme comprised of Shoc2/SurB and the catalytic subunit of PP1 functions as an M-Ras effector to modulate Raf activity. *Mol. Cell* **22**, 217–230 (2006).
- 18 Corceddu, V., Di Schiavi, E., Pennacchio, L. A., Ma'ayan, A., Sarkozy, A., Fodale, V. et al. Mutation of SHOC2 promotes aberrant protein N-myristoylation and causes Noonan-like syndrome with loose anagen hair. *Nat. Genet.* **41**, 1022–1026 (2009).
- 19 Makita, Y., Narumi, Y., Yoshida, M., Niihori, T., Kure, S., Fujieda, K. et al. Leukemia in cardio-facio-cutaneous (CFC) syndrome: a patient with a germline mutation in BRAF proto-oncogene. *J. Pediatr. Hematol. Oncol.* **29**, 287–290 (2007).
- 20 Ohtake, A., Aoki, Y., Saito, Y., Niihori, T., Shibuya, A., Kure, S. et al. Non-Hodgkin lymphoma in a patient with cardio-facio-cutaneous syndrome. *J. Pediatr. Hematol. Oncol.* (e-pub ahead of print 2 June 2010).
- 21 Armour, C. M. & Allanson, J. E. Further delineation of cardio-facio-cutaneous syndrome: clinical features of 38 individuals with proven mutations. *J. Med. Genet.* **45**, 249–254 (2008).
- 22 Narumi, Y., Aoki, Y., Niihori, T., Neri, G., Cave, H., Verloes, A. et al. Molecular and clinical characterization of cardio-facio-cutaneous (CFC) syndrome: overlapping clinical manifestations with Costello syndrome. *Am. J. Med. Genet. A* **143A**, 799–807 (2007).
- 23 Kobayashi, T., Aoki, Y., Niihori, T., Cave, H., Verloes, A., Okamoto, N. et al. Molecular and clinical analysis of RAF1 in Noonan syndrome and related disorders: dephosphorylation of serine 259 as the essential mechanism for mutant activation. *Hum. Mutat.* **31**, 284–294 (2010).
- 24 Tosti, A. & Piraccini, B. M. Loose anagen hair syndrome and loose anagen hair. *Arch. Dermatol.* **138**, 521–522 (2002).
- 25 Mazzanti, L., Cacciani, E., Cicognani, A., Bergamaschi, R., Scarano, E. & Forabosco, A. Noonan-like syndrome with loose anagen hair: a new syndrome? *Am. J. Med. Genet. A* **118A**, 279–286 (2003).
- 26 Tosti, A., Misciali, C., Borrello, P., Fanti, P. A., Bardazzi, F. & Patrizi, A. Loose anagen hair in a child with Noonan's syndrome. *Dermatologica* **182**, 247–249 (1991).
- 27 Flotho, C., Batz, C., Hasle, H., Bergstrasser, E., van den Heuvel-Eibrink, M. M., Zecca, M. et al. Mutational analysis of SHOC2, a novel gene for Noonan-like syndrome, in JMML. *Blood* **115**, 913 (2010).

Supplementary Information accompanies the paper on Journal of Human Genetics website (<http://www.nature.com/jhg>)

Case report

Cardio-facio-cutaneous syndrome with infantile spasms and delayed myelination

Koichi Aizaki^a, Kenji Sugai^a, Yoshiaki Saito^{a,*}, Eiji Nakagawa^a, Masayuki Sasaki^a,
Yoko Aoki^b, Yoichi Matsubara^b

^a Department of Child Neurology, National Center Hospital, National Center of Neurology and Psychiatry (NCNP), 4-1-1 Ogawahigashi-cho, Kodaira, Tokyo 187-8551, Japan

^b Department of Medical Genetics, Tohoku University School of Medicine, 1-1 Seiryomachi, Sendai 980-8574, Japan

Received 14 January 2010; received in revised form 25 February 2010; accepted 23 March 2010

Abstract

A girl with cardio-facio-cutaneous (CFC) syndrome due to a *BRAF* gene mutation (c.1454T→C, p.L485S) experienced repetitive epileptic spasms at the corrected age of 4 months. Electroencephalograms revealed hypsarrhythmia, and magnetic resonance imaging identified delayed myelination and a hypoplastic corpus callosum. Various antiepileptic treatments, including adrenocorticotropic hormone therapy, were ineffective, although transient seizure control was achieved by a ketogenic diet and clonazepam dipotassium. However, seizures with epileptic foci at the bilateral posterior temporal areas re-aggravated and remained intractable; severe psychomotor delay persisted. This case indicated that infantile spasms in CFC syndrome can be difficult to control and may be accompanied by severe psychomotor retardation and abnormal myelination.

© 2010 The Japanese Society of Child Neurology. Published by Elsevier B.V. All rights reserved.

Keywords: Cardio-facio-cutaneous syndrome; Infantile spasms; *BRAF*; Abnormal myelination

1. Introduction

Cardio-facio-cutaneous (CFC) syndrome is characterized by a distinctive facial appearance, congenital heart defects, ectodermal abnormalities, and psychomotor retardation [1]. *BRAF*, *MEK1*, *MEK2*, and *KRAS*, which are involved in the RAS/mitogen-activated protein kinase (MAPK) pathway, have been identified as the causative genes for CFC syndrome. The RAS-MAPK pathway is essential in regulation of the cell cycle, differentiation, growth, and cell senescence [2]. In particular, *BRAF* mutants are the most common in CFC syndrome; their gene product is highly expressed in the brain and plays

important roles in myelination and hippocampus-dependent learning [3,4].

A few recent reports have focused on the neurological symptoms of CFC syndrome, describing the complication of epilepsy and neuroradiological findings in this entity [5,6]. However, detailed information on individual patients, including the treatment course of epilepsy, has not been provided. We here describe a CFC syndrome patient with a *BRAF* gene mutation, who experienced infantile spasms and showed delayed myelination on magnetic resonance imaging (MRI).

2. Case report

A girl was born to nonconsanguineous Japanese parents at 33 weeks of gestation after a pregnancy complicated by polyhydramnios. There was no family history of epilepsy or neuromuscular disease and no previous

* Corresponding author. Tel.: +81 42 341 2711; fax: +81 42 346 1705.

E-mail address: saitoyo@ncnp.go.jp (Y. Saito).

pregnancy with spontaneous abortion. Birth weight was 2360 g (+2.1 SD), height 42 cm (−0.1 SD), and head circumference 32 cm (+1.7 SD). The Apgar score was 2 at 1 min and 6 at 5 min, and the patient needed artificial ventilation for several days. Mild laryngomalacia was noted, and cardiac ultrasonography revealed pulmonary valve stenosis, hypertrophic cardiomyopathy, and atrial septal defect. G-band analysis showed a karyotype of 46,XX. Metabolic screening tests of blood amino acids and urine organic acids showed negative results.

The patient was fed by a nasogastric tube because of poor milk intake. Repetitive brief tonic seizures emerged at the corrected age of 2 months and consisted of extension of the trunk, accompanied by staring and a few seconds of ocular bobbing. Asynchronous, high-voltage slow waves with multifocal sharp waves appeared with bilateral parieto-occipital predominance on interictal electroencephalogram (EEG) (Fig. 1A). The epileptic seizures remained intractable despite treatment with valproic acid and vitamin B6. Subsequently, the seizure type changed to tonic spasms in clusters when hypsarrhythmia was noted on EEG. Zonisamide (ZNS), clobazam (CLB), phenobarbital, and adrenocorticotropic

hormone (ACTH) therapy (0.01 mg/kg/day for 2 weeks) were also ineffective.

On physical examination at the corrected age of 4 months, her weight was 3950 g (−3.5 SD), height 59 cm (−1.2SD), and head circumference 36 cm (−3.4 SD). She presented with a prominent forehead; a coarse face; a wide, depressed nasal bridge with broad anteverted nares; thick lips; and low-set ears. Her hair was sparse and curly, and cutaneous findings included eczema of the face, skin redundancy in the proximal extremities, and deep palmar and plantar creases. Based on her characteristic facial appearance and cardiac anomalies, CFC syndrome was suspected. The patient manifested with generalized hypotonia and showed scarce responses to auditory or visual stimuli and no purposeful movements of the extremities. Deep tendon reflexes were normal. She did not smile or vocalize during this period and showed continuous laryngeal stridor. Laboratory findings revealed hypogammaglobulinemia but were otherwise unremarkable. MRI of the brain revealed a hypoplastic corpus callosum with moderate brain atrophy, delayed myelination, and an ambiguous corticomedullary boundary in the right posterior temporal lobe (Fig. 2A–C). Magneto-

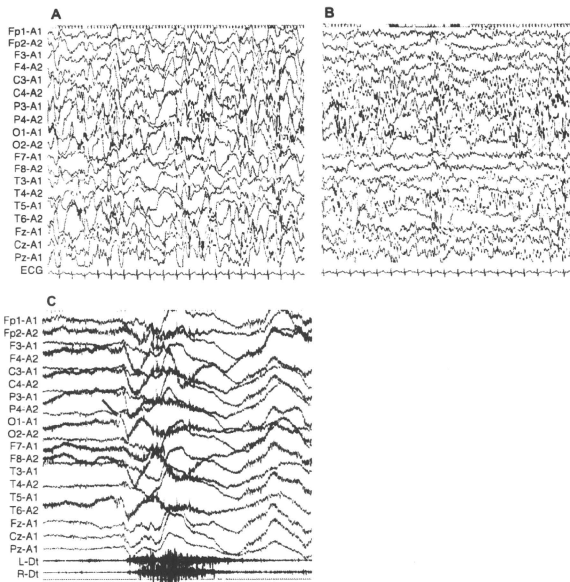


Fig. 1. Electroencephalograms (EEG) of the patient. (A and B) Interictal sleep EEG at the corrected ages of 5 (A) and 9 (B) months. (C) Ictal EEG of epileptic spasms at the corrected age of 5 months. L-Di, left deltoid muscle; R-Di, right deltoid muscle.

encephalography identified dipole sources at the bilateral temporo-parietal areas (Fig. 2D). Ictal EEG identified isolated spikes over the right parieto-occipital areas, which heralded the onset of repetitive epileptic spasms (Fig. 1C). Relative hyperperfusion was noted in the left temporo-parietal cortex on interictal single-photon emission computed tomography (SPECT) (Fig. 2E), and subtraction ictal SPECT coregistered to MRI during an episode of brief tonic seizure suggested an epileptic focus in the left temporal cortex (Fig. 2F).

Replacement of ZNS and CLB with potassium bromide (50 mg/kg/day) and topiramate (20 mg/kg/day) and re-administration of ACTH (up to 0.025 mg/kg/day) at the corrected age of 7 months did not improve seizure control. Tonic spasms with oculoccephalic deviation in series gradually increased to 10 times per day, and continuous oxygen supply was needed because of recurrent airway infection and increased salivation with frequent desaturation. After initiation of a ketogenic diet with a ketogenic ratio of 3:1 in combination with 0.3 mg/kg/day clorazepate dipotassium, epileptic seizures decreased in frequency by the fifth day and temporarily disappeared at the corrected age of 9 months. Partial improvement in the EEG findings (Fig. 1B) was noted during this period. Her respiratory condition also improved, and thus, oxygen therapy could be terminated. Body weight gradually increased to 6 kg in parallel with improvement in the general condition. However, her development was still stagnated and MRI (Fig. 2A–C) did not show any progress

in myelination. Seizures were exacerbated 1 month later and remained intractable.

Based on molecular studies, the patient was finally diagnosed with CFC syndrome. Genetic testing for mutations in *BRAF*, *MEK1*, *MEK2*, *KRAS*, and *HRAS* was performed, and a heterozygous *BRAF* gene mutation (c.1454T→C, p.L485S) was identified.

3. Discussion

Intellectual disabilities in CFC syndrome are more severe than those in Noonan and Costello syndromes, which are also caused by mutations in the constituents of the RAS/MAPK pathway [5,6]. However, the marked developmental delay in the present patient was more serious than that in usual cases of this entity [6]. This may be attributed to the complication of infantile spasms in this patient; the prevalence of this complication in CFC syndrome has been reported to be approximately 10% in large series [5,6]. Clinical information on these previous cases is very limited, and this is the first report on the detailed course of treatment for epileptic encephalopathy. This needs to be recognized to better understand the pathomechanism and management of this syndrome. In the central nervous system, *BRAF* is most densely expressed in hippocampal neurons [4], where the product of this gene is critically involved in the process of long-term potentiation and learning [7]. This preferential distribution may account for the severe psychomotor

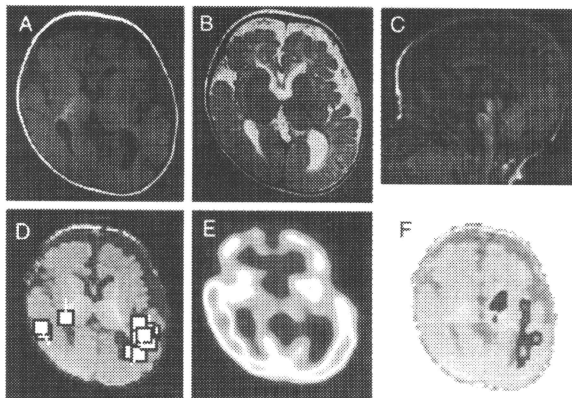


Fig. 2. Neuroimaging of the patient. (A–C) Magnetic resonance images at the corrected age of 9 months. Myelination is visible in the posterior limb of the internal capsule, optic radiation, and deep white matter of the frontal lobe (A and C, T1-weighted images; B, T2-weighted image), which corresponds to the pattern of early infancy. (D–F) examined at the corrected age of 5 months) Magnetic electroencephalogram (D), interictal single-photon emission computed tomography (SPECT) (E), and subtraction of ictal SPECT coregistered to MRI (F) based on a brief tonic seizure.

retardation in CFC syndrome, but the role of this genetic defect in epileptogenesis remains unclear. The presence of brain anomalies, including pachygyria and heterotopia, in CFC syndrome supports the contribution of *BRAF* to the morphogenesis of the brain and may be partly responsible for epilepsy in CFC syndrome. The ambiguous corticomedullary boundary in the right temporal lobe in the present patient may represent cortical dysgenesis in this area, which may have played a role in the evolution of infantile spasms in this patient. We observed another patient with a *BRAF* mutation (c.1495A→G, p.G499E) and lobar dysplasia in the left temporal cortex [8] (initially reported as Noonan syndrome). This suggests a propensity toward involvement of this region in CFC syndrome, possibly through the specific spatial distribution of the *BRAF* gene in corticogenesis and epileptogenesis. Although abundant *BRAF* expression in the fetal cerebrum has been confirmed, further studies on the detailed distribution of this gene in cell populations and cortical regions are required [9].

Another characteristic of the present patient was markedly delayed myelination throughout the course of the disease. Nonspecific delayed myelination and thinning of the corpus callosum are not uncommon findings in infantile spasms, which may be related to the persistence of hypersarhythmic discharges [10]. However, these findings have also been recognized in some CFC syndrome patients without infantile spasms [5]. Conditional ablation of the *BRAF* gene in neuroglial precursors in mice resulted in severe dysmyelination and defective oligodendrocyte differentiation [3], thus supporting the idea that CFC syndrome can be regarded as a type of myelination disorder. Given that the presence of delayed myelination does not always correlate with seizure control and developmental outcomes in infantile spasms [11], the significance of this MRI finding in epileptogenesis and prognosis of CFC syndrome should be specifically explored.

Another patient with CFC syndrome due to an L485S mutation in the *BRAF* gene, identical to the defect in the present case, also showed infantile spasms [5]. This mutated residue is located in the protein kinase domain, a defect of which would critically affect the

activity of *BRAF* protein. Although some mutations in this domain could result in a less severe phenotype [5], the neurological complications observed in the present patient, i.e., epileptic encephalopathy and abnormal myelination, may be specifically linked to certain genetic defects in CFC syndrome and may be characteristic in patients with a severe phenotype. Further analysis of genotype–phenotype correlations is required in this regard.

References

- [1] Niihori T, Aoki Y, Narumi Y, Neri G, Cavé H, Verloes A, et al. Germline *KRAS* and *BRAF* mutations in cardio-facio-cutaneous syndrome. *Nat Genet* 2006;38:294–6.
- [2] Aoki Y, Niihori T, Narumi Y, Kure S, Matsubara Y. The *RAS*/MAPK syndromes: novel roles of the *RAS* pathway in human genetic disorders. *Hum Mutat* 2008;29:992–1006.
- [3] Galabova-Kovacs G, Catalanotti F, Malzen D, Reyes GX, Zezula J, Herbst R, et al. Essential role of B-raf in oligodendrocyte maturation and myelination during postnatal central nervous system development. *J Cell Biol* 2008;180:947–55.
- [4] Di Benedetto B, Hitz C, Höller SM, Kühn R, Vogt Weisenhorn DM, Wurst W. Differential mRNA distribution of components of the ERK/MAPK signaling cascade in the adult mouse brain. *J Comp Neurol* 2007;500:542–56.
- [5] Yoon G, Rosenberg J, Blaser S, Rauen KA. Neurological complications of cardio-facio-cutaneous syndrome. *Dev Med Child Neurol* 2007;49:894–9.
- [6] Armour CM, Allanson JE. Further delineation of cardio-facio-cutaneous syndrome: clinical features of 38 individuals with proven mutations. *J Med Genet* 2008;45:249–54.
- [7] Morozov A, Muzzio IA, Bourtschouladze R, Van Strien N, Lapidus K, Yin D, et al. Rap1 couples cAMP signaling to a distinct pool of p42/44MAPK regulating excitability, synaptic plasticity, learning, and memory. *Neuron* 2003;39(2):309–25.
- [8] Saito Y, Sasaki M, Hanaoka S, Sugai K, Hashimoto T. A case of Noonan syndrome with cortical dysplasia. *Pediatr Neurol* 1997;17:266–9.
- [9] Storm SM, Cleveland JL, Rapp UR. Expression of raf family proto-oncogenes in normal mouse tissues. *Oncogene* 1990;5:345–51.
- [10] Saltik S, Koer N, Derwent A. Magnetic resonance imaging findings in infantile spasms: etiologic and pathophysiologic aspects. *J Child Neurol* 2003;18:241–6.
- [11] Takano T, Hayashi A, Sokoda T, Sawai C, Sakaue Y, Takeuchi Y. Delayed myelination at the onset of cryptogenic West syndrome. *Pediatr Neurol* 2007;37:417–20.

ORIGINAL ARTICLE

A genome-wide association study identifies *RNF213* as the first Moyamoya disease gene

Fumiaki Kamada¹, Yoko Aoki¹, Ayumi Narisawa^{1,2}, Yu Abe¹, Shoko Komatsuzaki¹, Atsuo Kikuchi³, Junko Kanno¹, Tetsuya Niihori¹, Masao Ono⁴, Naoto Ishii⁵, Yuji Owada⁶, Miki Fujimura², Yoichi Mashimo⁷, Yoichi Suzuki⁷, Akira Hata⁷, Shigeru Tsuchiya³, Teiji Tominaga², Yoichi Matsubara¹ and Shigeo Kure^{1,3}

Moyamoya disease (MMD) shows progressive cerebral angiopathy characterized by bilateral internal carotid artery stenosis and abnormal collateral vessels. Although ~15% of MMD cases are familial, the MMD gene(s) remain unknown. A genome-wide association study of 785 720 single-nucleotide polymorphisms (SNPs) was performed, comparing 72 Japanese MMD patients with 45 Japanese controls and resulting in a strong association of chromosome 17q25-ter with MMD risk. This result was further confirmed by a locus-specific association study using 335 SNPs in the 17q25-ter region. A single haplotype consisting of seven SNPs at the *RNF213* locus was tightly associated with MMD ($P=5.3 \times 10^{-10}$). *RNF213* encodes a really interesting new gene finger protein with an AAA ATPase domain and is abundantly expressed in spleen and leukocytes. An RNA *in situ* hybridization analysis of mouse tissues indicated that mature lymphocytes express higher levels of *Rnf213* mRNA than their immature counterparts. Mutational analysis of *RNF213* revealed a founder mutation, p.R4859K, in 95% of MMD families, 73% of non-familial MMD cases and 1.4% of controls; this mutation greatly increases the risk of MMD ($P=1.2 \times 10^{-43}$, odds ratio=190.8, 95% confidence interval=71.7–507.9). Three additional missense mutations were identified in the p.R4859K-negative patients. These results indicate that *RNF213* is the first identified susceptibility gene for MMD.

Journal of Human Genetics (2011) 56, 34–40; doi:10.1038/jhg.2010.132; published online 4 November 2010

INTRODUCTION

'Moyamoya' is a Japanese expression for something hazy, such as a puff of cigarette smoke drifting in the air. In individuals with Moyamoya disease (MMD), there is a progressive stenosis of the internal carotid arteries; a fine network of collateral vessels, which resembles a puff of smoke on a cerebral angiogram, develops at the base of the brain (Figure 1a).^{1,2} This steno-occlusive change can cause transient ischemic attacks and/or cerebral infarction, and rupture of the collateral vessels can cause intracranial hemorrhage. Children under 10 years of age account for nearly 50% of all MMD cases.³

The etiology of MMD remains unclear, although epidemiological studies suggest that bacterial or viral infection may be implicated in the development of the disease.⁴ Growing attention has been paid to the upregulation of arteriogenesis and angiogenesis associated with MMD because chronic ischemia in other disease conditions is not always associated with a massive development of collateral vessels.^{5,6} Several angiogenic growth factors are thought to have functions in the development of MMD.⁷

Several lines of evidence support the importance of genetic factors in susceptibility to MMD.⁸ First, 10–15% of individuals with MMD

have a family history of the disease.⁹ Second, the concordance rate of MMD in monozygotic twins is as high as 80%.¹⁰ Third, the prevalence of MMD is 10 times higher in East Asia, especially in Japan (6 per 100 000 population), than in Western countries.³ Familial MMD may be inherited in an autosomal dominant fashion with low penetrance or in a polygenic manner.¹¹ Linkage studies of MMD families have revealed five candidate loci for an MMD gene: chromosomes 3p24–26,¹² 6q25,¹³ 8q13–24,¹⁰ 12p12–13¹⁰ and 17q25.¹⁴ However, no susceptibility gene for MMD has been identified to date.

We collected 20 familial cases of MMD to investigate linkage in the five putative MMD loci. However, a definitive result was not obtained for any of the loci. We then hypothesized that there might be a founder mutation among Japanese patients with MMD because the prevalence of MMD is unusually high in Japan.¹⁵ Genome-wide and locus-specific association studies were performed and successfully identified a single gene, *RNF213*, linked to MMD. We report here a strong association between MMD onset and a founder mutation in *RNF213*, as well as the expression profiles of *RNF213*, in various tissues.

¹Department of Medical Genetics, Tohoku University School of Medicine, Sendai, Japan; ²Department of Neurosurgery, Tohoku University School of Medicine, Sendai, Japan; ³Department of Pediatrics, Tohoku University School of Medicine, Sendai, Japan; ⁴Department of Pathology, Tohoku University School of Medicine, Sendai, Japan; ⁵Department of Microbiology and Immunology, Tohoku University School of Medicine, Sendai, Japan; ⁶Department of Organ Anatomy, Yamaguchi University Graduate School of Medicine, Ube, Japan and ⁷Department of Public Health, Graduate School of Medicine, Chiba University, Chiba, Japan
 Correspondence: Dr S Kure, Department of Pediatrics, Tohoku University School of Medicine, 1-1 Seiryō-nachi, Aoba-ku, Miyagi, Sendai 980-8574, Japan.
 E-mail: kure@med.tohoku.ac.jp

Received 30 September 2010; accepted 1 October 2010; published online 4 November 2010

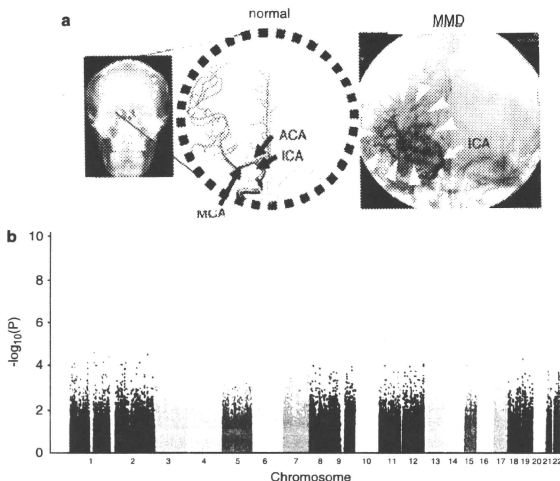


Figure 1 (a) Abnormal brain vessels in MMD. The dotted circle indicates the X-ray field of cerebral angiography (left panel). Normal structures of the right internal carotid artery (ICA), anterior cerebral artery (ACA) and middle cerebral artery (MCA) are illustrated (middle panel). The arrowheads indicate abnormal collateral vessels appearing like a puff of smoke in the angiogram of an individual with MMD (right panel). Note that ACA and MCA are barely visible, because of the occlusion of the terminal portion of the ICA. (b) Manhattan plot of the 785 720 SNPs used in the genome-wide association analysis of MMD patients. Note that the SNPs in the 17q25-ter region reach a significance of $P < 10^{-6}$.

MATERIALS AND METHODS

Affected individuals

Genomic DNA was extracted from blood and/or saliva samples obtained from members of the families with MMD (Supplementary Figure 1), MMD patients with no family history and control subjects. All of the subjects were Japanese. MMD was diagnosed on the basis of guidelines established by the Research Committee on Spontaneous Occlusion of the Circle of Willis of the Ministry of Health and Welfare of Japan. This study was approved by the Ethics Committee of Tohoku University School of Medicine. Total RNA samples were purified from leukocytes using an RNeasy mini kit (Qiagen, Hilden, Germany) and used as templates for cDNA synthesis with an Oligo (dT)₂₀ primer and SuperScript II reverse transcriptase according to the manufacturer's instructions (Invitrogen, Carlsbad, CA, USA).

Linkage analysis

For the linkage analysis, DNA samples were genotyped for 36 microsatellite markers within five previously reported MMD loci using the ABI 373A DNA Sequencer (Applied Biosystems, Foster City, CA, USA). Pedigrees and haplotypes were constructed with the Cyrillic version 2.1 software (Oxfordshire, UK). Multipoint analyses were conducted using the GENEHUNTER 2 software (<http://www.broadinstitute.org/ftp/distribution/software/genehunter/>). Statistical analysis was performed with SPSS version 14.0J (SPSS, Tokyo, Japan).

Genome-wide and locus-specific association studies

A genome-wide association study was performed using a group of 72 MMD patients, which consisted of 64 patients without a family history of MMD and 8 probands of MMD families. The Illumina Human Omni-Quad 1 chip (Illumina, San Diego, CA, USA) was used for genotyping, and single-nucleotide polymorphisms (SNPs) with a genotyping completion rate of 100% were used for further statistical analysis (785 720 out of 1 140 419 SNPs). Genotyping data

from 45 healthy Japanese controls were obtained from the database at the International HapMap Project web site. The 785 720 SNPs were statistically analyzed using the PLINK software (<http://pngu.mgh.harvard.edu/~purcell/plink/index.shtml>). For a locus-specific association study, we used 63 DNA samples consisting of 58 non-familial MMD patients and 5 probands of MMD families. A total of 384 SNPs within chromosome 17q25-ter were genotyped (Supplementary Table 1), using the GoldenGate Assay and a custom SNP chip (Illumina). Genotyping data for 45 healthy Japanese were used as a control. Case-control single-marker analysis, haplotype frequency estimation and significance testing of differences in haplotype frequency were performed using the Haploview version 3.32 program (<http://www.broad.mit.edu/mpg/haploview/>).

Mutation detection

Mutational analyses of *RNF213* and *FLJ35220* were performed by PCR amplification of each coding exon and putative promoter regions, followed by direct sequencing. Genomic sequence data for the two genes were obtained from the National Center for Biotechnology Information web site (<http://www.ncbi.nlm.nih.gov/>) for design of exon-specific PCR primers. *RNF213* cDNA fragments were amplified from leukocyte mRNA for sequencing analysis. Sequencing of the PCR products was performed with the ABI BigDye Terminator Cycle Sequencing Reaction Kit using the ABI 310 Genetic Analyzer. Identified base changes were screened in control subjects. Statistical difference of the carrier frequency of each base change was estimated by Fisher's exact test (the MMD group vs the control group).

Quantitative PCR

MTC Multiple Tissue cDNA Panels (Clontech Laboratory, Madison, WI, USA) were the source of cDNAs from human cell lines, adult and fetal tissues. Mononuclear cells and polymorphonuclear cells were isolated from the fresh peripheral blood of healthy human adults using Polymorphprep (Cosmo Bio,

Carlsbad, CA, USA). T and B cells were isolated from the fresh peripheral blood of healthy human adults using the autoMACS separator (Miltenyi Biotec, Bergisch Gladbach, Germany). Total RNA was isolated from these cells with the RNeasy Mini Kit (Qiagen) following the manufacturer's instructions. We reverse transcribed 100 ng samples of total RNA into cDNAs using the High Capacity cDNA Reverse Transcription Kit (Applied Biosystems). Quantitative PCRs were performed in a final volume of 20 μ l using the FastStart TaqMan Probe Master (Roche) (Roche, Madison, WI, USA), 5 μ l of cDNA, 10 μ M of RNF- or GAPDH-specific primers and 10 μ M of probes (Universal ProbeLibrary Probe #80 for RNF213 and Roche Probe #60 for GAPDH). All reactions were performed in triplicate using the ABI 7500 Real-Time PCR system (Applied Biosystems). Cycling conditions were 2 min at 50°C and 10 min at 95°C, followed by 40 cycles of 15 s at 95°C and 60 s at 60°C. Real-time PCR data were analyzed by the SDS version 1.2.1 software (Applied Biosystems). We evaluated the relative level of RNF213 mRNA by determining the C_T value, the PCR cycle at which the reporter fluorescence exceeded the signal baseline. GAPDH mRNA was used as an internal reference for normalization of the quantitative expression values.

Multiplex PCR

MTC Multiple Tissue cDNA Panels (Clontech) were the source of human cell lines and cDNAs from human adult and fetal tissues. Multiplex PCRs were performed in a final volume of 20 μ l using the Multiplex PCR Master Mix (Qiagen), 2 μ l of cDNA, a 2 μ M concentration of RNF213 and a 10 μ M concentration of GAPDH-specific primers. The samples were separated on a 2% agarose gel stained with ethidium bromide. Cycling conditions were 15 min at 94°C, followed by 30 cycles of 30 s at 94°C, 30 s at 57°C and 30 s at 72°C. For normalization of the expression levels, we used GAPDH as an internal reference for each sample.

In situ hybridization (ISH) analysis

Paraffin-embedded blocks and sections of mouse tissues for ISH were obtained from Genostaff (Tokyo, Japan). The mouse tissues were dissected, fixed with Tissue Fixative (Genostaff), embedded in paraffin by proprietary procedures (Genostaff) and sectioned at 6 μ m. To generate anti-sense and sense RNA probes, a 521-bp DNA fragment corresponding to nucleotide positions 470–990 of mouse Rnf213 (BC038025) was subcloned into the pGEM-T Easy vector (Promega, Madison, WI, USA). Hybridization was performed with digoxigenin-labeled RNA probes at concentrations of 300 ng ml⁻¹ in Probe Diluent-1 (Genostaff) at 60°C for 16 h. Coloring reactions were performed with NBT/BCIP solution (Sigma-Aldrich, St Louis, MO, USA). The sections were counterstained with Kernechtrot stain solution (Mutoh, Tokyo, Japan), dehydrated and mounted with Mallinol (Mutoh). For observation of Rnf213 expression in activated lymphocytes, 10-week-old Balb/c mice were intraperitoneally injected with 100 μ g of keyhole limpet hemocyanin and incomplete adjuvant and sacrificed in 2 weeks. The spleen of the mice was removed for Hematoxylin–eosin staining and ISH analysis.

RESULTS

Using 20 Japanese MMD families, we reevaluated the linkage mapped previously to five putative MMD loci. No locus with significant linkage, Lod score > 3.0 or NPL score > 4.0 was confirmed (Supplementary Figure 2). We conducted a genome-wide association study of 72 Japanese MMD cases. Single-marker allelic tests comparing the 72 MMD cases and 45 controls were performed for 785 720 SNPs using χ^2 statistics. These tests identified a single locus with a strong association with MMD ($P < 10^{-8}$) on chromosome 17q25-ter (Figure 1b), which is in line with the latest mapping data of a MMD locus.¹⁶ The SNP markers with $P < 10^{-6}$ are listed in Table 1. To confirm this observation, we performed a locus-specific association study. A total of 384 SNP markers (Supplementary Table 1) were selected within the chromosome 17q25-ter region and genotyped in a set of 63 MMD cases and 45 controls. The SNP markers demonstrating a high association with MMD ($P < 10^{-6}$) were clustered in a 151-kb region from base position 75 851 399–76 003 020 (SNP No.116–136 in

Table 1 A genome-wide association study of Japanese MMD patients and controls

1	SNP	Chromosome	Base position	Gene	Risk allele/ non-risk allele	Risk allele frequency in MMD	Risk allele frequency in controls	χ^2	P-value	Odds ratio	95% confidence interval	
											Lower	Upper
1	rs11870849	17	76 025 668	RNF213	T/C	0.4792	0.1111	33.55	6.95E-09	7.36	3.532	15.34
2	rs6565661	17	75 965 089	RNF213	A/G	0.7361	0.3667	31.35	2.16E-08	4.819	2.733	8.489
3	rs7216493	17	75 941 933	RNF213	G/A	0.75	0.3889	30.39	3.53E-08	4.715	2.673	8.313
4	rs7217421	17	75 850 055	RNF213	A/G	0.6667	0.3	29.86	4.64E-08	4.666	2.642	8.237
5	rs124449863	17	75 857 806	RNF213	C/T	0.6667	0.3	29.86	4.64E-08	4.666	2.642	8.237
6	rs4890009	17	75 926 103	RNF213	G/A	0.8819	0.5778	28.5	9.38E-08	5.459	2.831	10.527
7	SNP17-75933731	17	75 933 731	RNF213	G/A	0.6819	0.5778	28.5	9.38E-08	5.458	2.831	10.527
8	rs7219131	17	75 867 365	RNF213	T/C	0.8819	0.3111	28.11	1.15E-07	4.429	2.517	7.794
9	rs6565677	17	75 932 037	RNF213	T/C	0.7431	0.3977	27.43	1.63E-07	4.378	2.483	7.722
10	rs4889848	17	75 969 256	RNF213	C/T	0.735	0.4111	26.99	2.05E-07	4.297	2.444	7.889
11	rs7224239	17	75 869 771	RNF213	A/G	0.6661	0.3667	26.99	2.05E-07	5.03	2.659	9.529

Abbreviations: MMD, moyamoya disease; SNP, single-nucleotide polymorphism. A genome-wide association study testing 1 140 419 SNPs on the Human Omni-Quad chip (Illumina, San Diego, CA, USA) was performed in 72 Japanese MMD cases. Single-marker allelic tests between the cases and controls were performed using χ^2 statistics for all markers. This table lists the 11 SNP markers with a significance of $P < 10^{-6}$.

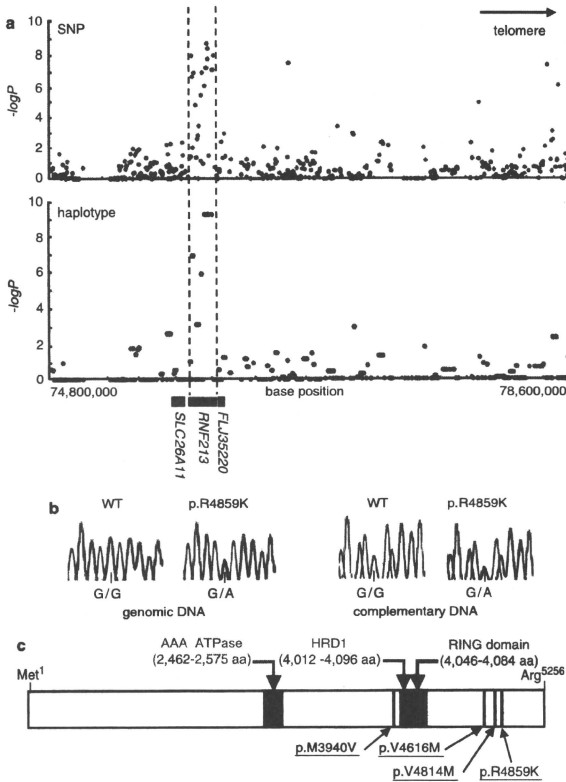


Figure 2 (a) Association analysis of 63 non-familial MMD cases and 45 control subjects. Statistical significance was evaluated by the χ^2 -test. SNP markers with a strong association with MMD ($P < 10^{-6}$) clustered in a 161-kb region (base position 75 851 399–76 012 838) indicated by two dotted lines (upper panel), which included the entire region of *RNF213* (lower panel). Haplotype analysis revealed a strong association ($P = 5.3 \times 10^{-10}$) between MMD and a single haplotype located within *RNF213*. (b) Sequencing chromatograms of the identified MMD mutations. The left panel shows the sequences of an unaffected individual and a carrier of a p.R4859K heterozygous mutation. The right panel indicates the sequencing chromatograms of the leukocyte cDNA obtained from an unaffected individual and an individual with MMD who carries the p.R4859K mutation. Note that both wild-type and mutant alleles were expressed in leukocytes. (c) The structure of the RNF213 protein. The RNF213 protein contains three characteristic structures, the AAA-superfamily ATPase motif, the RING motif and the HMG-CoA reductase degradation motif. The positions of four mutations identified in MMD patients are underlined, including one prevalent mutation (red) and three private mutations (black).

Supplementary Table 1); this entire region was within the *RNF213* locus (Figure 2a). A single haplotype determined by seven SNPs (SNP Nos.130–136 in Supplementary Table 1) that resided in the 3' region of *RNF213* was strongly associated with MMD onset ($P = 5.3 \times 10^{-10}$). Analysis of the linkage disequilibrium block indicated that this haplotype was not in complete linkage disequilibrium with any other haplotype in this region (Supplementary Figure 3). These results strongly suggest that a founder mutation may exist in the 3' part of *RNF213*.

Mutational analysis of the entire coding and promoter regions of *RNF213* and *FLJ35220*, a gene 3' adjacent to *RNF213*, revealed that 19 of the 20 MMD families shared the same single base substitution, c.14576G>A, in exon 60 of *RNF213* (Figure 2b and Table 2). This nucleotide change causes an amino-acid substitution from arginine⁴⁸⁵⁹ to lysine⁴⁸⁵⁹ (p.R4859K). The p.R4859K mutation was identified in 46 of 63 non-familial MMD cases (73%), including 45 heterozygotes and a single homozygote (Table 3). Both the wild-type and the p.R4859K mutant alleles were co-expressed in leukocytes

Table 2 Nucleotide changes with amino-acid substitutions identified in the sequencing analysis of *RNF213* and *FLJ35220*

Gene	Exon	Nucleotide change ^a (amino-acid substitution)	Genotype (allele)			P-value ^b	χ^2 (df=1) ^c	Odds ratio (95% CI)
			Non-familial cases	Control subjects				
<i>RNF213</i>	29	c.7809C > A (p.D2603E)	2/63 (2/126)	15/381 (15/762)	0.77	0.09	0.80 (0.2–3.6)	
<i>RNF213</i>	41	c.11818A > G (p.M3940V)	1/63 (1/126)	0/388 (0/776)	0.01	6.17	ND	
<i>RNF213</i>	41	c.11891A > G (p.E3964G)	4/63 (4/126)	3/55 (4/110)	0.84	0.04	1.2 (0.3–5.5)	
<i>RNF213</i>	52	c.13342G > A (p.A4448T)	4/63 (4/126)	2/53 (2/106)	0.53	0.39	1.7 (0.3–9.8)	
<i>RNF213</i>	56	c.13846G > A (p.V4616M)	1/63 (1/126)	0/388 (0/776)	0.01	6.17	ND	
<i>RNF213</i>	59	c.14440G > A (p.V4814M)	1/63 (1/126)	0/388 (0/776)	0.01	6.17	ND	
<i>RNF213</i>	60	c.14576G > A (p.R4859K)	46/63 (47/126)	6/429 (6/858)	1.2 × 10 ⁻⁴³	298.1	190.8 (71.7–507.9)	
<i>FLJ35220</i>		None						

Abbreviations: ND, not determined; SNP, single-nucleotide polymorphism.

^aNucleotide numbers of *RNF213* cDNA are counted from the A of the ATG initiator methionine codon (NCBI Reference sequence, NP_065965.4).

^bP-values were calculated by Fisher's exact test.

^cGenotypic distribution (carrier of the polymorphism vs non-carrier).

Table 3 Association of the p.R4859K (c.14576G > A) mutation with MMD

	Total	Genotype		
		wt/wt (%)	wt/p.R4859K (%)	p.R4859K/p.R4859K (%) ^d
Members of 19 MMD families^a				
Affected	42	0	39 (92.9)	3 (7.1)
Not affected	28	15 (53.6)	13 (46.4)	0
Individuals without a family history of MMD^{b,c}				
Affected	63	17 (27.0)	45 (71.4)	1 (1.6)
Not affected	429	423 (98.6)	6 (1.4)	0

Abbreviations: MMD, moyamoya disease.

^aEntire distribution, $\chi^2=29.4$, $P=4.2 \times 10^{-7}$.

^bEntire distribution, $\chi^2=298.2$, $P=1.8 \times 10^{-65}$.

^cGenotypic distribution (p.R4859K carrier vs non-carrier), $\chi^2=298.1$, $P=1.2 \times 10^{-43}$, odds ratio=190.8 (95% CI=71.7–507.9).

^dThe age of onset and initial symptoms of the four homozygotes were comparable to those of the 84 heterozygous patients.

in three patients heterozygous for the p.R4859K mutation (Figure 2b), excluding the possible instability of the mutant *RNF213* mRNA. Additional missense mutations, p.M3940V, p.V4616M and p.V4814M, were detected in three non-familial MMD cases without the p.R4859K mutation (Figure 2c). These mutations were not found in 388 control subjects and were detected in only one patient, suggesting that they were private mutations (Table 2). No copy number variation or mutation was identified in the *RNF213* locus of 12 MMD patients using comparative genome hybridization microarray analysis (Supplementary Figure 4). In total, 6 of the 429 control subjects (1.4%) were found to be heterozygous carriers of p.R4859K. Therefore, we concluded that the p.R4859K mutation increases the risk of MMD by a remarkably high amount (odds ratio=190.8 (95% confidence interval=71.7–507.9), $P=1.2 \times 10^{-43}$) (Table 3). It was recently reported that an SNP (rs161110142) in the promoter region of *RPTOR*, which is located ~150 kb downstream from *RNF213*, was associated with MMD.¹⁷ Genotyping of the SNP in *RPTOR* showed that the *RNF213* p.R4859K mutation was more strongly associated with MMD than rs161110142 (Supplementary Figure 1).

RNF213 encodes a protein with 5256 amino acids harboring a RING (really interesting new gene) finger motif, suggesting that it

functions as an E3 ubiquitin ligase (Figure 2c). It also has an AAA ATPase domain, which is characteristic of energy-dependent unfoldases.¹⁸ To our knowledge, *RNF213* is the first RING finger protein known to contain an AAA ATPase domain. The expression profile of *RNF213* has not been previously fully characterized. We performed a quantitative reverse transcription PCR analysis in various human tissues and cells. *RNF213* mRNA was highly expressed in immune tissues, such as spleen and leukocytes (Figure 3a and Supplementary Figure 5). Expression of *RNF213* was detected in fractions of both polymorphonuclear cells and mononuclear cells and was found in both B and T cell fractions (Supplementary Figure 6). A low but significant expression of *RNF213* was also observed in human umbilical vein endothelial cells and human pulmonary artery smooth muscle cells. Cellular expression was not enhanced in tumor cell lines, compared with leukocytes. In human fetal tissues, the highest expression was observed in leukocytes and the thymus (Supplementary Figure 6E). The expression of *RNF213* was surprisingly low in both adult and fetal brains. Overall, *RNF213* was ubiquitously expressed, and the highest expression was observed in immune tissues.

We studied the cellular expression of *Rnf213* in mice. The ISH analysis of spleen showed that *Rnf213* mRNA was present in small mononuclear cells, which were mainly localized in the white pulps (Figures 3b–g). The ISH signals were also detected in the primary follicles in the lymph node and in thymocytes in the medulla of the thymus (Supplementary Figure 7). To study *Rnf213* expression in activated lymphocytes we immunized mice with keyhole limpet hemocyanin, and examined *Rnf213* mRNA in spleen by ISH analysis. Primary immunization with keyhole limpet hemocyanin antigen revealed that the expression of *Rnf213* in the secondary follicle is as high as in the primary follicle in the lymph node (Supplementary Figure 8). In an E16.5 mouse embryo, expression was observed in the medulla of the thymus and in the cells around the mucous palatine glands (Supplementary Figure 9). These findings suggest that mature lymphocytes in a static state express *Rnf213* mRNA at a higher level than do their immature counterparts.

DISCUSSION

We identified a susceptibility locus for MMD by genome-wide and locus-specific association studies. Further sequencing analysis revealed a founder missense mutation in *RNF213*, p.R4859K, which was tightly associated with MMD onset. Identification of a founder mutation in individuals with MMD would resolve the following recurrent

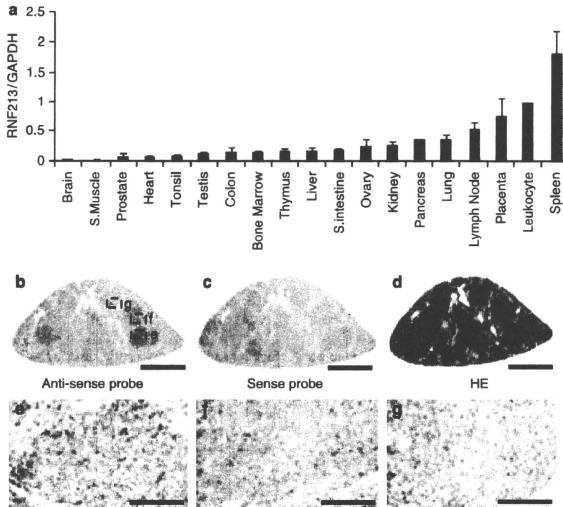


Figure 3 Expression of human RNF213 and murine Rnf213. (a) RT-PCR analysis of RNF213 mRNA in various human tissues. The expression levels of RNF213 mRNA in various adult human tissues were evaluated by quantitative PCR using GAPDH mRNA as a control. The signal ratio of RNF213 mRNA to GAPDH mRNA in each sample is shown on the vertical axis. (b-g) *In situ* hybridization (ISH) analysis of Rnf213 mRNA in mouse spleen. Specific signals for Rnf213 mRNA were detected by ISH analysis with the anti-sense probe (b) but not with the sense probe (c). Hematoxylin-eosin staining of the mouse spleen (d). Signals for the Rnf213 mRNA were observed in small mononuclear cells, which were mainly localized in the white pulps (dotted square, e) and partially distributed in the red pulps (dotted squares, f and g). Panels e, f and g show the high-magnification images of the corresponding fields in panel b. Scale bars, 1 mm (b-d) and 50 μ m (e-g).

questions:^{2,19} (i) why is MMD more prevalent in East Asia than in Western countries? The carrier frequency of p.R4859K in Japan is 1/72 (Table 2). In contrast, we found no p.R4859K carrier in 400 Caucasian controls (data not shown). Furthermore, no mutation was identified in five Caucasian patients with MMD after the full sequencing of RNF213. These results suggest that the genetic background of MMD in Asian populations is distinct from that in Western populations and that the low incidence of MMD in Western countries may be attributable to a lack of the founder RNF213 mutation. (ii) Is unilateral involvement a subtype of MMD or a different disease?² We collected DNA samples from six patients with unilateral involvement and found a p.R4859K mutation in four of them (data not shown), suggesting that bilateral and unilateral MMD share a genetic background. (iii) Is pre-symptomatic diagnosis of MMD possible? In the present study, MMD never developed in the 15 mutation-negative family members in the 19 MMD families with the p.R4859K mutation (Table 3 and Supplementary Figure 1), suggesting the feasibility of pre-symptomatic diagnosis or exclusion by genetic testing.

How the mutant RNF213 protein causes MMD remains to be elucidated. The expression of RNF213 was more abundant in a subset of leukocytes than in the brain, suggesting that blood cells have a function in the etiology of MMD. This observation agrees with a previous report that MMD patients have systemic angiopathy.²⁰

Recent studies have suggested that the postnatal vasculature can form through vasculogenesis, a process by which endothelial progenitor cell are recruited from the splenic pool and differentiate into mature endothelial cells.²¹ Levels of endothelial progenitor cells in the peripheral blood are increased in MMD patients.²² RNF213 may be expressed in splenic endothelial progenitor cells and mutant RNF213 might dysregulate the function of the endothelial progenitor cells. Further research is necessary to elucidate the role of RNF213 in the etiology of MMD.

CONFLICT OF INTEREST

The authors declare no conflict of interest.

ACKNOWLEDGEMENTS

We thank all of the patients and their families for participating in this study. We also thank Dr Hidetoshi Ikeda at the Department of Neurosurgery, Tohoku University School of Medicine and Drs Toshiaki Hayashi and Reizo Shirane at the Department of Neurosurgery, Miyagi Children's Hospital, Sendai, Japan for patient recruitment. We are grateful to Ms Kumi Kato for technical assistance. This study was supported by grants from the Ministry of Education, Culture, Sports, Science and Technology, Japan and by the Research Committee on Moyamoya Disease of the Ministry of Health, Labor and Welfare, Japan.

- 1 Suzuki, J. & Takaku, A. Cerebrovascular 'moyamoya' disease. Disease showing abnormal net-like vessels in base of brain. *Arch. Neurol.* **20**, 288–299 (1969).
- 2 Suzuki, J. *Moyamoya Disease* (Springer-Verlag: Berlin, 1983).
- 3 Oki, K., Hoshino, H. & Suzuki, N. In: *Moyamoya Disease Update*, (eds Cho B.K., Tominaga T.) 29–34 (Springer: New York, 2010).
- 4 Phi, J. H., Kim, S. K., Wang, K. C. & Cho, B. K. In: *Moyamoya Disease Update*, (eds Cho B.K., Tominaga T.) 82–86, (Springer: New York, 2010).
- 5 Yoshihara, T., Taguchi, A., Matsuyama, T., Shimizu, Y., Kikuchi-Taura, A., Soma, T. *et al.* Increase in circulating CD34-positive cells in patients with angiographic evidence of moyamoya-like vessels. *J. Cereb. Blood Flow Metab.* **28**, 1086–1089 (2008).
- 6 Achrol, A. S., Guzman, R., Lee, M. & Steinberg, G. K. Pathophysiology and genetic factors in moyamoya disease. *Neurosurg. Focus* **26**, E4 (2009).
- 7 Scott, R. M. & Smith, E. R. Moyamoya disease and moyamoya syndrome. *N. Engl. J. Med.* **360**, 1226–1237 (2009).
- 8 Kure, S. In: *Moyamoya Disease Update* (eds Cho B.K., Tominaga T.) 41–45 (Springer: Tokyo, 2010).
- 9 Kuriyama, S., Kusaka, Y., Fujimura, M., Wakai, K., Tamakoshi, A., Hashimoto, S. *et al.* Prevalence and clinicoepidemiological features of moyamoya disease in Japan: findings from a nationwide epidemiological survey. *Stroke* **39**, 42–47 (2008).
- 10 Sakurai, K., Horiuchi, Y., Ikeda, H., Ikezaki, K., Yoshimoto, T., Fukui, M. *et al.* A novel susceptibility locus for moyamoya disease on chromosome 8q23. *J. Hum. Genet.* **49**, 278–281 (2004).
- 11 Namba, R., Kuroda, S., Tada, M., Ishikawa, T., Houkin, K. & Iwasaki, Y. Clinical features of familial moyamoya disease. *Childs. Nerv. Syst.* **22**, 258–262 (2006).
- 12 Ikeda, H., Sasaki, T., Yoshimoto, T., Fukui, M. & Arinami, T. Mapping of a familial moyamoya disease gene to chromosome 3p24.2-p26. *Am. J. Hum. Genet.* **64**, 533–537 (1999).
- 13 Inoue, T. K., Ikezaki, K., Sasazuki, T., Matsushima, T. & Fukui, M. Linkage analysis of moyamoya disease on chromosome 6. *J. Child. Neurol.* **15**, 179–182 (2000).
- 14 Yamauchi, T., Tada, M., Houkin, K., Tanaka, T., Nakamura, Y., Kuroda, S. *et al.* Linkage of familial moyamoya disease (spontaneous occlusion of the circle of Willis) to chromosome 17q25. *Stroke* **31**, 930–935 (2000).
- 15 Wakai, K., Tamakoshi, A., Ikezaki, K., Fukui, M., Kawamura, T., Aoki, R. *et al.* Epidemiological features of moyamoya disease in Japan: findings from a nationwide survey. *Clin. Neurol. Neurosurg.* **99**(Suppl 2), S1–S5 (1997).
- 16 Mineharu, Y., Liu, W., Inoue, K., Matsuura, N., Inoue, S., Takenaka, K. *et al.* Autosomal dominant moyamoya disease maps to chromosome 17q25.3. *Neurology* **70**, 2357–2363 (2008).
- 17 Liu, W., Hashikata, H., Inoue, K., Matsuura, N., Mineharu, Y., Kobayashi, H. *et al.* A rare Asian founder polymorphism of Raptor may explain the high prevalence of Moyamoya disease among East Asians and its low prevalence among Caucasians. *Environ. Health Prev. Med.* **15**, 94–104 (2010).
- 18 Lupas, A. N. & Martin, J. AAA proteins. *Curr. Opin. Struct. Biol.* **12**, 746–753 (2002).
- 19 Ikezaki, K. In: *Moyamoya disease* (eds Ikezaki K., Loftus C. M.) 43–75 (Thieme: New York, 2001).
- 20 Ikeda, E. Systemic vascular changes in spontaneous occlusion of the circle of Willis. *Stroke* **22**, 1358–1362 (1991).
- 21 Zampetaki, A., Kirton, J. P. & Xu, Q. Vascular repair by endothelial progenitor cells. *Cardiovasc. Res.* **78**, 413–421 (2008).
- 22 Rafat, N., Beck, G., Pena-Tapia, P. G., Schmiedek, P. & Vajkoczy, P. Increased levels of circulating endothelial progenitor cells in patients with Moyamoya disease. *Stroke* **40**, 432–438 (2009).

Supplementary Information accompanies the paper on Journal of Human Genetics website (<http://www.nature.com/jhg>)

Implications of Prenatal Diagnosis of the Fetus With Both Interstitial Deletion and a Small Marker Ring Originating From Chromosome 5

Hiroyasu Ohashi,¹ Kaoru Suzumori,^{1,2*} Yasushi Chisaka,³ Shinichi Sonta,¹ Tomoko Kobayashi,⁴ Yoko Aoki,⁴ Yoichi Matsubara,⁴ Michiko Sone,⁵ and Lisa G. Shaffer⁶

¹Fetal Life Science Center, Ltd., Nagoya, Japan

²Department of Obstetrics and Gynecology, Nagoya City University, Nagoya, Japan

³Department of Obstetrics and Gynecology, Tohoku University, Sendai, Japan

⁴Department of Medical Genetics, Tohoku University, Sendai, Japan

⁵Kagawa National Children's Hospital, Zentsuji, Kagawa, Japan

⁶Signature Genomic Laboratories, Spokane, Washington

Received 5 May 2010; Accepted 2 August 2010

We describe a patient with 47,XY,del(5)(p11p13), +mar observed in prenatal screening. We performed analyses including G-banding, multi-color fluorescent in situ hybridization (mFISH) for fetal chromosome detection. After birth array-based comparative genomic hybridization (aCGH), bacterial artificial chromosome (BAC)-FISH was carried out to define the chromosomal changes precisely. The mFISH revealed that a ring chromosome that had originated from chromosome 5. The aCGH showed that this fetus had a terminal duplication, an interstitial deletion, and a pericentromeric duplication of the short arm of chromosome 5. This complex alteration resulted in partial trisomy 5p15.33–p15.31, partial monosomy 5p14.3–p13.2, and partial trisomy 5p12–p11. To clarify these alterations, we performed BAC-FISH using BAC clones related to deleted and duplicated regions, and found that a derivative (der) chromosome 5 showed the presence of hybridization signals from the duplicated region at 5p15.33 and the loss of hybridization signals from the deleted region at 5p14.2. In addition, FISH analysis confirmed the origin of the marker chromosome. Hybridization signals from the second intervening sequence at 5p13.1, between the deleted region and the pericentric duplicated region, were present on the marker ring chromosome. © 2010 Wiley-Liss, Inc.

Key words: BAC-FISH; microarray analysis; prenatal diagnosis; ring chromosome

INTRODUCTION

When genetic abnormalities are observed during prenatal screening, deletions, and supernumerary ring chromosomes are often seen separately [Gardner and Sutherland, 1996; Ryan et al., 1997; Slavotinek and Kingston, 1997]. Most cases with deletion of autosomes, even that of a tiny segment, are accompanied by clinical symptoms, including mental and developmental retardation; on

How to Cite this Article:

Ohashi H, Suzumori K, Chisaka Y, Sonta S, Kobayashi T, Aoki Y, Matsubara Y, Sone M, Shaffer LG. 2011. Implications of prenatal diagnosis of the fetus with both interstitial deletion and a small marker ring originating from chromosome 5.

Am J Med Genet Part A 155:192–196.

the other hand, there have been examples of cases with deletion of autosomes without any abnormal features [Gardner and Sutherland, 1996; Daniel and Malafej, 2003; Liehr et al., 2004].

Here, we describe a rare case with both interstitial deletion and a small ring originating from the same chromosome 5 detected prenatally and characterized by molecular cytogenetics. We emphasize the usefulness of molecular cytogenetics involving array-based comparative genomic hybridization (aCGH) and bacterial artificial chromosome (BAC)-fluorescent in situ hybridization BAC-FISH in providing precise information in cases of complex structural abnormality.

CLINICAL REPORT

Amniocentesis requested for advanced maternal age was performed in gestational week 16 on a 42-year-old woman with two

*Correspondence to:

Kaoru Suzumori, M.D., Ph.D., Fetal Life Science Center, 2-22-8 Chikusa, Chikusa-Ku, Nagoya 464-0858, Japan. E-mail: k.suzumori@flsc.jp
Published online 22 December 2010 in Wiley Online Library (wileyonlinelibrary.com).

DOI 10.1002/ajmg.a.33764

normal children. Fetal chromosomes were analyzed by GTG banding and multi-color fluorescent in situ hybridization (mFISH) using cultured amniocytes. After cytogenetic analyses, she was informed that one chromosome 5 with interstitial deletion and a small marker ring chromosome were detected in all the cells. Then, chromosomal analysis of the parents was performed on peripheral blood and showed normal karyotypes. It was difficult to offer additional molecular analyses within a limited term for pregnancy interruption. Ultrasonographic examination at 19 weeks of gestation did not detect any specific abnormality in the fetus. Despite possible unfavorable prognosis informed in genetic counseling, she and her spouse decided against termination of the pregnancy.

The pregnancy was uneventful and she delivered a phenotypically normal boy at 39 weeks of gestation. Apgar score was 8/8 and there were no particular clinical features. Body length, weight, and head circumference were within the normal range: 48 cm, 2,916 g, and 33 cm, respectively. After birth, we received informed consent to examine aCGH and BAC-FISH for further confirmation of the diagnosis.

Developmental, physical, and neurological examinations were normal and he appropriately reached his milestones. At 1 year and 6 months, his developmental quotient (DQ) was 110 (Fig. 1); echocardiography and brain imaging were also normal.

MULTICOLOR CYTOGENETIC STUDIES

Chromosome and FISH Analyses

Cultured amniocytes were analyzed using G-banding with 540 bands per haploid number. G-banded chromosomes demonstrated

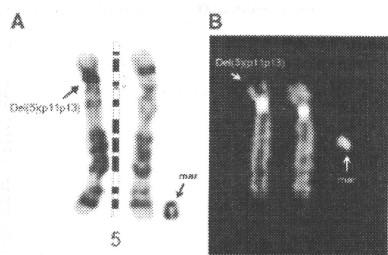


FIG. 2. Partial karyogram of chromosome 5, del(5p), and supernumerary ring by G-banding (A) and mFISH (B).

that all cells had an interstitial deletion of chromosome 5 (5p11 → p13), and a small marker ring chromosome (Fig. 2A). The origin of this marker chromosome was unclear by G-banding. Therefore, the initial karyotyping was 47,XY,del(5)(p11p13), +mar. The mFISH revealed that the marker ring originated from chromosome 5, the same as the deleted chromosome (Fig. 2B). The ring chromosome seemed to have a centromere because this marker was detected in all cells. Chromosome analysis of the parents showed no abnormalities, indicating that these structural abnormalities in the fetus were de novo.

Oligonucleotide aCGH

For detection of gain and loss of chromosome segments, oligonucleotide-based microarray analysis was performed on reserved cultured amniocytes using a 105K-feature whole-genome microarray (Signature Chip Oligo Solution[®], made for Signature Genomic Laboratories by Aligent Technologies Inc., Santa Clara, CA) [Ballif et al., 2008]. Microarray analysis of 1543 loci using an oligonucleotide array detected a complex abnormality in the DNA obtained from cultured amniocytes. Based on microarray analysis, this fetus had two duplications and a deletion of the short arm of chromosome 5. This abnormality was first characterized by a single copy gain of 380 oligonucleotide probes from the terminal end of the short arm of 5p, at 5p15.33p15.31. The extent of this duplication has been estimated to be approximately 6.1 Mb. The second alteration was characterized by a single copy loss of 347 oligonucleotide probes from 5p14.3p13.2. The extent of this interstitial deletion is estimated to be approximately 15.3 Mb. The third alteration was characterized by a single copy gain of 147 oligonucleotide probes from the pericentric region at 5p12p11. The extent of this duplication has been estimated to be approximately 3.4 Mb. Thus, this complex alteration resulted in partial trisomy 5p15.33–p15.31, partial monosomy 5p14.3–p13.2, and partial trisomy 5p12–p11. In conclusion, the result of microarray was arr5p15.33–p15.31(131,945–6,267,160)x3, 5p14.3–p13.2(21,438,495–36,736,934)x1, 5p12–p11(42,529,343–45,908,725)x3 (Fig. 3).



FIG. 1. Propositus at age 8 months (left picture) and 1 year 6 months (right picture). Note the phenotypically normal boy.

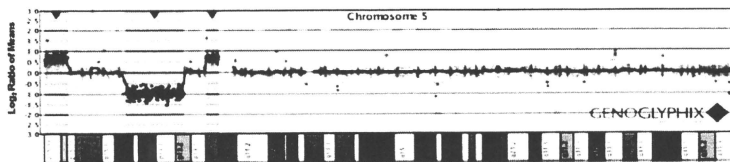


FIG. 3. Microarray plot showing, from left to right, a single copy gain of 380 oligonucleotide probes at 5p15.33p15.31, approximately 6.1 Mb in size; a single copy loss of 347 oligonucleotide probes from 5p14.3p13.2, approximately 15.3 Mb; and single copy gain of 147 oligonucleotide probes at 5p12p11, approximately 3.4 Mb in size. Probes are ordered on the x-axis according to physical mapping positions, with the distal p-arm on the left and the distal q-arm on the right.

BAC-FISH

For confirmation of the array results, FISH analyses were performed with BAC clones from duplicated and deleted regions as previously described [Shaffer et al., 1994; Traylor et al., 2009]. For this study, we used cord blood obtained at delivery.

FISH using a BAC clone from the 5p14.2 deleted region (RP11-701M20) and the 5p15.33 duplicated region (RP11-1006P13) identified an abnormal deleted (del) chromosome 5 that showed the loss of hybridization signals from the deleted region at 5p14.2 (Fig. 4A) and the presence of hybridization signals from the duplicated region at 5p15.33 (Fig. 4C). Interphase FISH

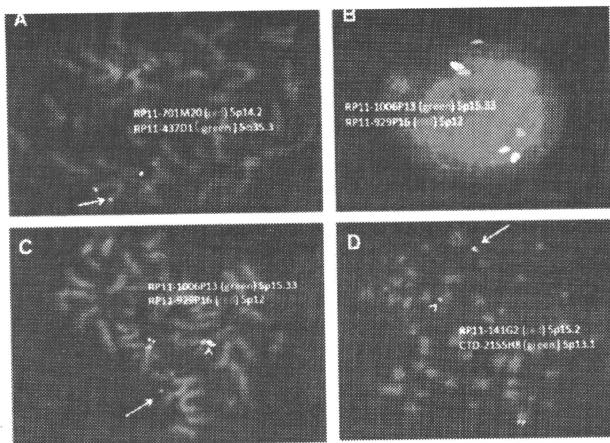


FIG. 4. FISH characterizations of a complex rearrangement on the short arm of chromosome 5. A: FISH showing a deletion of 5p14.2, BAC clone RP11-701M20 from 5p14.2 is labeled in red, and RP11-437D1 from 5q35.3 is labeled in green as a control. The presence of one red signal indicates deletion of 5p14.2 on one homologue (arrow). B, C: FISH with probes from the two regions is shown to be present in three copies by aCGH. BAC clone RP11-1006P13 from 5p15.33 is labeled in green, and RP11-929P16 from 5p12 is labeled in red. Interphase FISH [B] confirmed the presence of three copies of both regions. Metaphase FISH [C] shows a red signal but not a green signal on a small, supernumerary ring chromosome (arrow), indicating the presence of the 5p12 material on the supernumerary chromosome. Dotted green signals from 5p15.33 were present on the normal chromosome 5 homologs, but terminal duplicated signals were observed on one chromosome 5 (arrowhead). D: FISH with probes from the intervening regions shown to be present in two copies by aCGH. BAC clone RP11-141G2 from 5p15.2 is labeled in red, and CTD-2155H8 from 5p13.1 is labeled in green. The supernumerary ring chromosome (arrow) shows a green signal and therefore the presence of material from 5p13.1, while one chromosome 5 homolog (arrowhead) shows a deletion for this region. The probe from 5p15.2 shows a normal hybridization pattern.

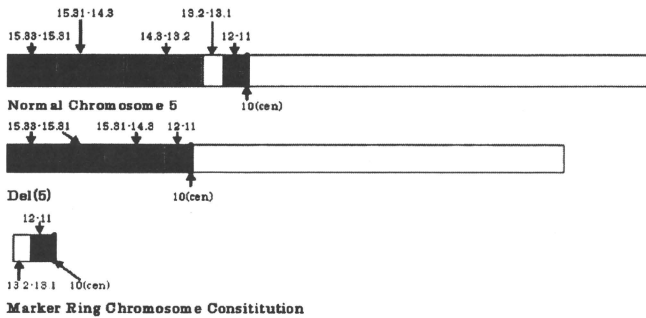


FIG. 5. Molecular background information on the deleted chromosome 5 and marker ring chromosome.

(Fig. 4B) clarified the presence of three copies of 5p15.33 and 5p12 regions. This del(5) also showed hybridization signals in an experiment using BAC clones from the first normal intervening sequence, between the terminal duplication and the deleted region, at 5p15.2 (RP11-141G2; Fig. 4D). Additional FISH analysis using a BAC clone from the 5p12 duplicated region (RP11-929P16) confirmed the origin of the marker ring chromosome (Fig. 4C). Hybridization signals from the second intervening normal sequence at 5p13.1 (CTD-2155H8), between the deleted region and the pericentric duplicated region, were also present on the marker ring chromosome, but not on the del(5), indicating that the deletion on that chromosome extends from 5p14.3 through 5p13.1 (Fig. 4D).

In conclusion, this baby had two abnormal derivative chromosomes. The first der(5) had an abnormal short arm with a duplication of 5p15.31 → 5p15.33, and a deletion of 5p13.1 → p14.3. The second der(5), the marker ring chromosome, was comprised of material from 5p10 → p13.2 (Fig. 5). The final karyotype of the baby is: 47,XY,ish der(5)(pter → p15.31::pter → p14.3::p11 → qter)(RP11-1006P13+,,RP11-141G2+,RP11-701M20–,CTD-2155H8–),+der(5):(13.2 → p10):(CTD-2155H8+,RP11-929P16+).

DISCUSSION

Partial deletion of 5p is often seen in prenatal diagnoses and newborn analyses [Mainardi et al., 2001; Weiss et al., 2003]. In autosomes other than chromosome 5, deletions involving various chromosomes have also been reported in the literature [Gardner and Sutherland, 1996; Ryan et al., 1997; Slavotinek and Kingston, 1997]. Partial deletion of autosomes is generally accompanied by mild-to-severe clinical symptoms, including mental and developmental retardation in babies, although there have been exceptional cases where no clinical symptoms are observed [Callen et al., 1993; Overhauser et al., 1994; Knight et al., 1995]. Supernumerary marker chromosomes including small rings are also seen frequently in prenatal diagnoses [Michalski et al., 1993; Brøndum-Nielsen and

Mikkelsen, 1995; Karaman et al., 2006]. Among babies with such small markers, some cases have no clinical features, but others showed mild-to-severe abnormalities after birth [Callen et al., 1993; Overhauser et al., 1994; Knight et al., 1995; Gardner and Sutherland, 1996; Daniel and Malafiej, 2003; Liehr et al., 2004; Bernardini et al., 2007]. Thus, in genetic counseling, it is important to offer chromosomal information from prenatal diagnoses and to provide as much detail as possible, including the origin and inheritance.

The present case had a deletion and a supernumerary marker ring chromosome. To our knowledge, this is the first report of detection by prenatal screening of both a deletion and a marker ring. In the literature, there are some mosaic cases of clones with a deletion and an additional ring separately [Gutiérrez-Angulo et al., 2002; Gereltzul et al., 2008; Kara et al., 2008], but such cases are extremely rare. In newborn infants, only one other case has been reported [Schuffenhauer et al., 1996] with a deletion and a ring of chromosome 5; this baby showed a mosaicism of 46,XY,del(5)/47,XY,del(5),+dic(5), with macrocephaly, asymmetric square skull, minor facial anomalies, omphalocele, inguinal hernias, hypospadias, and club feet. The break points of the deletion shared cen and p13 with those of the dicentric ring chromosome; this case had partial duplication of 5p (p13 → cen), and the mechanisms of del(5) and dic(5) were relatively straightforward. In the present case, on the other hand, the mechanisms of del(5) and marker ring [r(5)] were extremely complex. Microarray analysis revealed a terminal duplication, an interstitial deletion, and a pericentromeric duplication of the short arm of chromosome 5. Through this analysis, a total of six break points of the short arm of chromosome 5 (p15.33, p15.31, p14.3, p13.2, p12, and p11) were related to the formation of the structural abnormality with the duplication and the deletion, and the marker ring. According to the results of the G-band analysis of this case, we determined the break points of del(5) to be p11 and p13. However, assuming the microarray data are correct, the composition of r(5) becomes complicated, and explanation of the underlying mechanisms becomes difficult. To facilitate understanding of the exact composition of del(5) and r(5),

we performed FISH analysis using BAC clones from the duplicated 5p15.33, 5p12 regions and deleted 5p14.2 region. The short arm of the del(5) revealed a duplication of 5p15.31 → 5p15.33 and a deletion of 5p13.1 → p14.3. The r(5) was comprised of material from 5p10 → p13.2. Although supernumerary ring chromosome formation is difficult to determine, we speculate that this case have resulted from "centromere misdivision" along with a break in either the p or q arm, forming a small ring chromosome [Baldwin et al., 2008].

In summary, this complex 5p abnormality was characterized by a terminal duplication of 5p15.33p15.31 of approximately 6.4 Mb, an interstitial deletion 5p14.3p13.2 of approximately 15.3 Mb and an interstitial duplication of 5p12p11 of approximately 3.4 Mb. The 5p terminal duplication contained at least 21 genes including ADAMTS16, AHRH, and C5orf38. The 5p14.3p13.2 deletion lacked at least 22 genes including *CDH12*, *PRDM9*, *CDH10*, and *DH9*. The 5p12p11 duplication contained at least 11 genes including *GHR*, *SEPP1*, *C5orf39*, and *ZNF11131*.

When the child was examined at 1 year and 6 months, we could not find any developmental abnormality, either physical or mental. Because of his age he will need to be followed to confirm normal intellectual development. In order to provide accurate and useful genetic counseling in similar cases in the future, the accumulation of further reports with complicated chromosome abnormalities would be beneficial.

REFERENCES

- Baldwin EL, May LE, Justice AN, Martin CL, Ledbetter DH. 2008. Mechanism and consequences of small supernumerary marker chromosomes: From Barbara McClintock to modern genetic-counseling issue. *Am J Hum Genet* 82:398–410.
- Ballif BC, Theisen A, McDonald-McGinn DM, Zackai EH, Bejjani BA, Shaffer LG. 2008. Identification of a previously unrecognized microdeletion syndrome of 16q11.2q12.2. *Clin Genet* 74:469–475.
- Bernardini L, Capalbo A, D'Avanzo MG, Torrente I, Grammatico P, Dell'Edera D, Cavalcanti DP, Novelli A, Dallapiccola B. 2007. Five cases of supernumerary small ring chromosomes 1: Heterogeneity and genotype-phenotype correlation. *Eur J Med Genet* 50:94–102.
- Brøndum-Nielsen K, Mikkelsen M. 1995. A 10-year survey, 1980–1990, of prenatally diagnosed small supernumerary marker chromosomes, identified by FISH analysis. Outcome and follow-up of 14 cases diagnosed in a series of 12,699 prenatal samples. *Prenat Diagn* 15:615–619.
- Callen DF, Eyre H, Lane S, Shen Y, Hansmann I, Spinner N, Zackai E, McDonald-McGinn D, Schuffenhauer S, Wauters J, Van Thienen M-N, Van Roy B, Sutherland GR, Haan EA. 1993. High resolution mapping of interstitial long arm deletions of chromosome 16: Relationship to phenotype. *J Med Genet* 30:828–832.
- Daniel A, Malafiej P. 2003. A series of supernumerary small ring marker autosomes identified by FISH with chromosome probe arrays and literature review excluding chromosome 15. *Am J Med Genet Part A* 117A:212–222.
- Gardner RJM, Sutherland GR. 1996. *Chromosome Abnormalities and Genetic Counseling*. 2nd edition. New York, Oxford: Oxford University Press. pp. 1–478.
- Gereltzul E, Baba Y, Suda N, Shiga M, Inoue MS, Tsuji M, Shin I, Hirata Y, Ohyama K, Moriyama K. 2008. Case report of de novo dup(18p)/del(18q) and r(18) mosaicism. *J Hum Genet* 53:941–946.
- Gutiérrez-Angulo M, Lazalde B, Vasquez AI, Leal C, Corral E, Rivera H. 2002. del(X)(p22.1)/r(X)(p22.1q28) Dynamic mosaicism in a Turner syndrome patient. *Ann Genet* 45:17–20.
- Kara N, Okten G, Gunö SO, Saglam Y, Tasdemir HA, Pinarli FA. 2008. An epileptic case with mosaic ring chromosome 6 and 6q terminal deletion. *Epilepsy Res* 80:219–223.
- Karaman B, Aytan M, Yilmaz K, Toksoy G, Onal EP, Ghanbari A, Engur A, Kayserili H, Yuksel-Apak M, Basaran S. 2006. The identification of small supernumerary marker chromosomes; the experiences of 15,792 fetal karyotyping from Turkey. *Eur J Med Genet* 49:207–214.
- Knight LA, Yong MH, Tan M, Ng IS. 1995. Del(3)(p25.3) without phenotypic effect. *J Med Genet* 32:994–995.
- Liehr T, Claussen U, Starke H. 2004. Small supernumerary marker chromosomes (sSMC) in humans. *Cytogenet Genome Res* 107:55–67.
- Mainardi PC, Perfumo C, Cãli A, Coucourde G, Pastore G, Cavani S, Zara F, Overhauser J, Pierluigi M, Bricarelli FD. 2001. Clinical and molecular characterization of 80 patients with 5p deletion: Genotype-phenotype correlation. *J Med Genet* 38:151–158.
- Michalski K, Rauer M, Williamson N, Perszyk A, Hoo JJ. 1993. Identification, counselling, and outcome of two cases of prenatally diagnosed supernumerary small ring chromosomes. *Am J Med Genet* 46:88–94.
- Overhauser J, Huang X, Gersh M, Wilson W, McMahon J, Bengtsson U, Rojas K, Meyer M, Wasmuth JJ. 1994. Molecular and phenotypic mapping of the short arm of chromosome 5: Sublocalization of the critical region for the cri-du-chat syndrome. *Hum Mol Genet* 3:247–252.
- Ryan AK, Goodship JA, Wilson DI, Philip N, Levy A, Seidel H, Schuffenhauer S, Oechsler H, Belohradsky B, Prieur M, Aurias A, Raymond FL, Clayton-Smith J, Hatchwell E, McKeown C, Beemer FA, Dallapiccola B, Novelli G, Hurst JA, Ignatius J, Green AJ, Winter RM, Brueton L, Brøndum-Nielsen K, Stewart F, Van Essen T, Patton M, Paterson J, Scambler PJ. 1997. Spectrum of clinical features associated with interstitial chromosome 22q11 deletions: A European collaborative study. *J Med Genet* 34:798–804.
- Schuffenhauer S, Kobelt A, Daumer-Haas C, Löffler C, Müller G, Murken J, Meitinger T. 1996. Interstitial deletion 5p accompanied by dicentric ring formation of the deleted segment resulting in trisomy 5p13-cen. *Am J Med Genet* 65:56–59.
- Shaffer LG, McCaskill C, Han J-Y, Choo KHA, Cuttito DM, Donnafenel AE, Weiss L, Van Dyke DL. 1994. Molecular characterization of de novo secondary trisomy 13. *Am J Hum Genet* 55:968–974.
- Slavotinek A, Kingston H. 1997. Interstitial deletion of bands 4q12 → q13.1: Case report and review of proximal 4q deletions. *J Med Genet* 34:862–865.
- Traylor R, Fan Z, Ballif BC. 2009. Microdeletion of 6q16.1 encompassing EPHA7 in a child with mild neurological abnormalities and dysmorphic features: Case report. *Mol Cytogenet* 2:1–6.
- Weiss A, Shalev S, Weiner E, Sheiner Y, Shalev E. 2003. Prenatal diagnosis of 5p deletion syndrome following abnormally low maternal serum human chorionic gonadotropin. *Prenat Diagn* 23:572–574.

特集 臨床遺伝学の進歩と日常診療

【遺伝性疾患の臨床】

日常診療に必要な臨床遺伝学と遺伝カウンセリング

齋藤 加代子

別刷

日本医師会雑誌

第139巻・第3号

平成22(2010)年6月

キーワード●遺伝形式、遺伝カウンセリング、臨床遺伝専門医、遺伝子検査

■はじめに

分子遺伝学の進歩は、医療において疾患の原因遺伝子の同定、発症メカニズムの解明、治療法の開発などの進歩をもたらし、遺伝子変異により重症度の判定を下し、適切な治療の方針を立てることに貢献できるようになった。遺伝子検査が保険収載され、遺伝性疾患における診断のための遺伝子検査は、一般診療の診断プロセスに含まれはじめた。その際、まず必要となる遺伝医学的な説明は疾患の遺伝形式についてであり、一般診療に携わる者も、遺伝子検査・染色体検査を実施する場合には臨床遺伝の知識が要求される。

また、遺伝に関する説明や遺伝カウンセリングは、診断が確定したうえで、さらに継続して実施されることが必要である。Duchenne型筋ジストロフィーなどのX連鎖劣性遺伝性疾患、筋強直性ジストロフィーやハンチントン病などの常染色体優性遺伝性疾患では、患者の確定診断が家系全体の診断をも意味すること、次の世代にも発症者が出現する可能性があることから、家族や血縁者についても遺伝カウンセリングが求められることが少なくない。

■検査の説明時に、まず配慮をすること

検査を受ける患者本人に、意思決定能力が十

分でない場合には、その意思を代弁できる代話者に対して、疾患に関する医学的情報、遺伝形式、遺伝子検査の目的、検査の有用性と限界などについて分かりやすく十分な説明を行い、理解を得たうえで、その自由意思を尊重することが最も重要である。さらに、遺伝子検査・染色体検査の結果は本人のみならず、家族・血縁者にも関係することから、家族・血縁者への配慮をする。必要に応じて臨床遺伝専門医や認定遺伝カウンセラーなどの遺伝医学の専門家への紹介を行い、遺伝カウンセリングの機会を提供する用意があることを説明する。

■遺伝カウンセリングとは

「遺伝カウンセリング」について、UNESCOの「ヒト遺伝情報に関する国際宣言(2003)」第11条では、「健康に関わる重要な意味を持つ可能性がある遺伝学的検査(遺伝子検査・染色体検査)を行おうとする場合、当事者が遺伝カウンセリングを適切な方法で受けられるようにすべきである。遺伝カウンセリングは非指示的であり、文化的に適合したものであり、かつ当事者の最大の利益と一致したものであるべきである」としている¹⁾。

遺伝医学関連学会による「遺伝学的検査に関するガイドライン」²⁾でも、遺伝子検査における遺伝カウンセリングの重要性を述べている。遺

Clinical Genetics and Genetic Counseling in Clinical Practice

Kayoko Saito : Institute of Medical Genetics, Tokyo Women's Medical University

東京女子医科大学附属遺伝子医療センター所長・教授